AIAA 81-4057

Roughness Effects on Boundary-Layer Transition in a Nozzle Throat

A. Demetriades*
Montana State University, Bozeman, Mont.

A boundary-layer transition study was carried out in the throat region of the DeLaval nozzle of a supersonic wind tunnel. The study was motivated equally by the need to find thresholds for laminar boundary-layer flow in the tunnel walls when roughness is present and by the desire to simulate transition on roughened blunt bodies in supersonic and hypersonic flow. Detailed inviscid and viscous flow measurements were done from the low subsonic to the supersonic regions of the nozzle throat. The roughness was caused by attaching distributed roughness overlays on the nozzle surface. Transition, detected by hot-film anemometers, was found to move upstream as the flow Reynolds number and/or the roughness height increased. Cast in the coordinates of some of the empirical blunt-body transition correlations currently in use, the present transition data agree with the available blunt-body data when the nondimensional roughness exceeds unity and support the concept of a constant roughness Reynolds number for transition in that regime. At the lower roughness heights, the results show that the transition Reynolds number departs from the aforementioned correlations and approaches a limit insensitive to roughness but characteristic of the experimental facility.

Nomenclature

A,B,C = constant in Eq. (1)
k = roughness height
$\bar{k}$ = nondimensional roughness height $[(k/\theta)(T_e/T_w)]$
M = Mach number
p = Pressure
p_T = pitot pressure
Re' = unit Reynolds number, based on local properties
Re_θ = momentum Reynolds numbers $= Re'\theta$
$Re_{\theta T}$ = transition momentum Reynolds number
T = temperature
x = distance along the flow vector
y = distance normal to the nozzle surface
δ = boundary-layer thickness
θ = boundary-layer momentum thickness
μ = fluid viscosity
ρ = fluid density

Subscripts

B = at the beginning of transition
E = at the end of transition
0 = stagnation (supply) conditions
w = wall properties
s = smooth-wall properties
k = properties at the roughness height

I. Introduction

A GREAT deal of the validity of wind-tunnel experimentation depends on whether the boundary layer growing on the wind-tunnel sidewalls is laminar or turbulent. In supersonic and hypersonic facilities particularly, turbulence in the region from the DeLaval nozzle throat on, can produce effects invalidating the desired flow simulation.[1,2] Boundary-layer transition studies would therefore be invaluable for the throat regions of individual wind tunnels, especially in the hope of eventually uniting these studies into practical design predictions. Theoretical estimates of boundary-layer growth and transition, however, are difficult in nozzles because of the complexity of their local flowfield with its subsonic-transonic-supersonic history and large curvature and pressure gradient; while in most cases direct boundary-layer measurements are impossible because of the mechanical inaccessibility of the throat and its sensitivity to intrusion of the diagnostics.

Compounding this question are recent observations[35] that in addition to the usual sensitivity of the throat boundary layer to the freestream turbulence and the flow upstream history, the layer is also extremely sensitive to surface disturbances, such as roughness and wall cooling. Such observations are reminiscent of a class of similar findings for the boundary layer growing on blunt (e.g., hemispherical) bodies at supersonic and hypersonic speeds,[4-6] a topic receiving much current attention. Both types of flow feature an acceleration of the flow from a near standstill to supersonic speeds, driven by the same type of favorable pressure gradient over the same type of convex surface. In both cases, surface roughness and wall cooling displace the transition zone upstream. The present work was motivated by this similarity in the transition behavior, in the hope that findings with one configuration might benefit the understanding of the other. Although the blunt-body flow is not an exact counterpart of the nozzle flow, for instance, because of the abrupt turning of the streamlines due to the bow shock, its measurement is also very difficult and badly in need of a more convenient simulator; for example, transition Reynolds numbers on blunt bodies are usually inferred from surface heat transfer measurements and theoretically calculated boundary-layer properties.[4] Despite its unwieldy features, a nozzle boundary layer can be used to simulate its blunt-body counterpart provided that more concrete evidence than now available is found that the transition characteristics in these two flows are similar.

The present experiment, therefore, set out to crosscheck and quantify the findings of Ref. 3 and to compare its findings with data of boundary-layer transition on blunt-bodies. For this purpose the nozzle-throat region of the continuous supersonic wind tunnel at Aeronutronics (Division of the Ford Aerospace and Communications Communications Corp., Newport Beach, Calif.) was used, with overlays of random distributed roughness attached to encourage early transition onset. The experiment established criteria for admissible roughness characteristics before the boundary layer on this nozzle becomes turbulent and produced data

Received Dec. 26, 1979; revision received Sept. 15, 1980.

*Professor of Mechanical Engineering. Associate Fellow AIAA.

testing the possibility of simulating transition on a blunt body in high-speed flow.

II. Experiment Design

The experiment was designed to study the movement of transition in the region of a DeLaval nozzle throat, as affected by Reynolds number and nozzle surface roughness. At the outset, the actual measurement of the laminar boundary-layer properties preceding transition, as well as the characterization of the roughness, were fixed as important requirements. The former requirement involved the preparation of a "map" of the laminar boundary-layer properties as a function of distance along the nozzle and of the wind-tunnel supply conditions. Such a map could then be used to present the transition observations in the form of transition (momentum) Reynolds number vs the properly normalized roughness height. It should be stressed that the transition Reynolds number was formed using the momentum thickness over the smooth wall to enable comparison with similar data on blunt-bodies[4,5] that had been reduced using an identical scheme. Thus, the characterization of the smooth wall boundary layer, the characterization of the added roughness, and the transition observations with and without roughness formed three distinct series of measurements.

The measurements also required a particular type of wind-tunnel design, that coincided with the physical arrangement of the supersonic wind-tunnel at Aeronutronic. What was required was a nozzle throat with large curvature radius, good visibility, accessibility to diagnostic sensors, and resistance to flow interference when such sensors were present in the throat region. The boundary-layer edge Mach number M_e of interest ranged from 0 to about 2, while the roughness heights k of interest were those for which the parameter $\tilde{k} \equiv (k/\theta)(T_e/T_w)$, which has been used to correlate blunt-body transition,[4,5] was smaller than about 2. This would enable a check on whether the transition results obtained for blunt bodies could be duplicated in the nozzle throat, as well as obtain hitherto unavailable transition data in the range $0 \leq \tilde{k} < 1$.

III. Measurement of Boundary-Layer Growth

As noted previously, the major task involved measurements of the smooth-wall ($\tilde{k}=0$) boundary-layer growth. The wind-tunnel used fulfilled admirably the requirements of the previous section since the throat radius of curvature is 30 cm, which is large enough to allow convenient streamwise probing with diagnostic sensors. Two opposing sides of the two-dimensional flow channel consist of polished aluminum nozzle blocks, while the other two are optical windows of high-quality (Schlieren) glass. Each window spans the length of the test section, to allow viewing of the flow, the nozzle surfaces, and the immersed probes from the low-subsonic stations of the flow to beyond the supersonic diffuser inlet. This feature of the wind tunnel was a critical advantage because, as noted later, it overcame the usual problems of probing through and upstream of the nozzle throat.

The boundary-layer profiles were measured with a pitot probe in the manner shown on Fig. 1. Fine 0.01 cm diam steel tubing, acid-etched to a sharp lipped 0.005 cm diam opening, formed the tip of the probe, giving a resolution of 1:10-1:25 for the boundary layer probed ($\delta \simeq 0.05$-0.125 cm). Regarding viscous effects on the readings of this pitot tube, in the worst case examined the edge unit Reynolds number was of order $2 \times 10^4 \text{cm}^{-1}$, whereas important effects do not set in[7] (for incompressible flow) until the probe Reynolds number is of order 20. Resolution and freedom from viscous effects were satisfactory over most of the length of flow examined, but probably not so at the upstream end of this length as will be discussed subsequently,

Surveys across the boundary-layer were taken with this probe at $x = -8.3$, -5.59, -3.05, 0.51, 2.39, 4.93 and 7.47 cm from the throat, where $x=0$ denotes the throat itself ($M_e = 1$) along the midspan position of the lower nozzle block. As will be seen later, these survey stations covered the range $0.2 < M_e < 2.2$ and were done at 50 mm Hg abs. increments of the supply pressure p_0, at $T_0 = 313$K. The maximum edge unit Reynolds number range thus obtained was from $Re' = 2 \times 10^4$ to 14×10^4 cm^{-1}. The data matrix was truncated when needed to make sure that the survey for every pair (x, p_0) dealt only with a laminar boundary layer.

Positioning the probe at the stations just mentioned was done by mounting it at the forward end of a long, thin cantilevered strut parallel to the flow. The diameter of the strut was 0.64 cm, so that it could pass through the 1.8×8.13 cm plane of the throat by obstructing no more than 7% of its flow area. Long experience with this wind tunnel, substantiated by many different measurements,[8] has shown that neither local nor upstream flow interference is caused by such an obstruction. An elaborate system had to be set up, however, to ensure rigidity and precision of positioning of the probe strut especially when the latter was extended upstream of the throat. The system, pictured in Fig. 1, involved three independent electromechanical actuators which controlled the motion and position of the probe. One actuator provided motion along the x axis and a second actuator provided coarse y motion (precision of order 0.001 in. = 0.0025 cm). A third

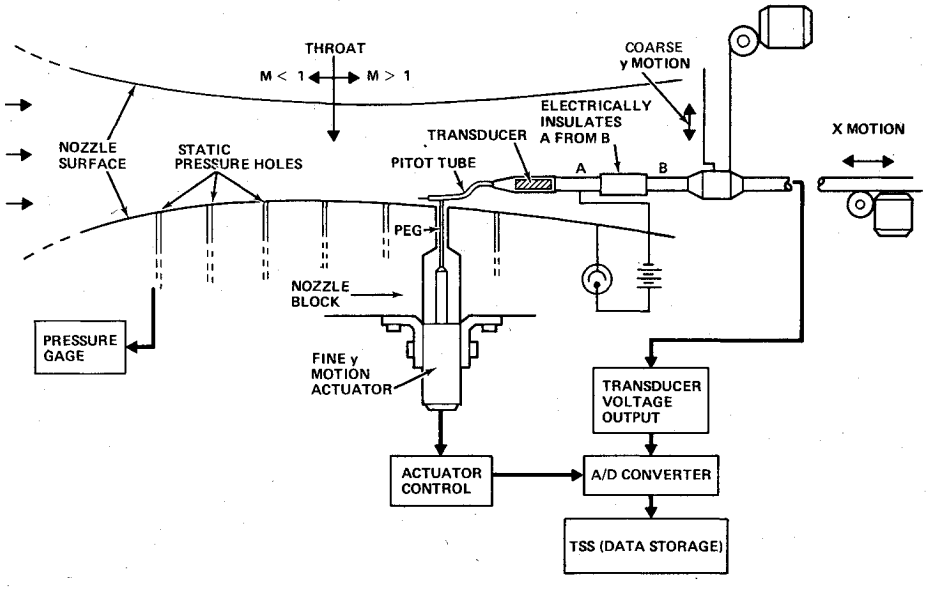

Fig. 1 Schematic of the experimental arrangement.

actuator played the dual role of providing support at the end of the cantilever and of positioning the probe tip with great accuracy. To this end a high-resolution (0.0001 in. or 0.00025 cm) actuator drove a 0.075 cm diam "peg" through each of the static pressure holes equidistantly located on the nozzle block surface. Since such a static orifice was located slightly downstream of each pitot survey station, the pitot tube could rigidly rest on and precisely be controlled by the actuator-driven peg as is shown on Fig. 2. A graticulated microscope was used to observe the pitot probe during each survey to ensure lack of vibration and to cross check the distance between the wall and the probe tip. For added accuracy, an indicator light, powered by a low-voltage circuit, was made to signal physical contact between the wall and the probe. A total of 70 boundary-layer pitot profiles were measured in this fashion for the values of x and p_0 chosen.

The static pressure over the smooth wall was also measured in the range $-8.13<x<7.47$ cm for $200<p_0<730$ mm Hg. These results agreed closely with the predictions of one-dimensional insentropic flow and were used to find the static pressure corresponding to each pitot survey. Furthermore, the flow was continuous and very close to adiabatic; for these conditions superficial estimates of the total temperature distribution through the layer are usually quite adequate.[9] In this case the wall recovery factor was taken at 0.9 and the total temperature was assumed to vary linearly across the layer. Using this variation and the measured pitot and static pressures, the point-by-point, edge, and integral properties of the laminar boundary layer were computed for each combination of x and p_0.

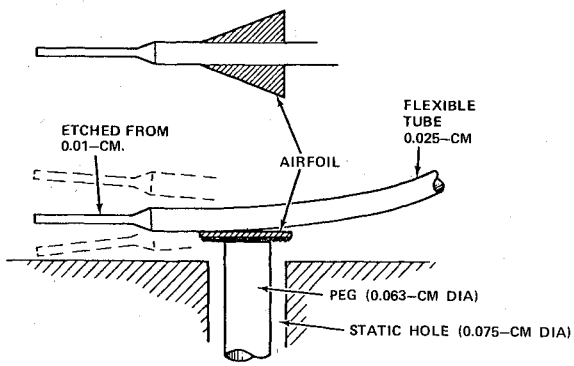

Fig. 2 Method of support and actuation of the pitot probe tip.

The results are typified by the variation of edge Mach and unit Reynolds numbers and of the momentum Reynolds number with x as shown on Figs. 3-5. The Mach number change through the throat as measured by two different combinations of p_{Te},p_0, and p_w are seen to be in fair-to-good agreement with the one-dimensional calculation; the differences, of course, are due to the theoretically expected inviscid-flow variation across the flow. The Re' vs x results of Fig. 4 are less sensitive to this variation and show the increasing-decreasing character of Re' which, incidentally, is also typical of flow over, say, hemispheres at high speeds.

Figure 5 shows the viscous flow results with the scatter of points reflecting scatter obtained in the measurement of θ, plots of which can be found in Ref. 10. Repeated measurements showed that the scatter could not be reduced, but that the layer thickness 1) remained nearly constant before the throat and increased rapidly past it and 2) at any station the thickness depended approximately on the inverse square root of p_0. The measured form factors δ/δ^* and δ/θ agreed,[10] within experimental error, with expectations from compressible laminar boundary-layer theory except at the most forward position. This is reflected on Fig. 5 as well, implying some problem with the measurement of θ in that position. This is not surprising considering earlier remarks on possible viscous and interference problems with the pitot probe in the forward position where δ is small. The $\theta(x,p_0)$ data were thus least-squares fitted into an analytic form, both for preventing the scatter in θ to artificially distort the transition data and for expediting the data reduction. As the best compromise between expectation and measurement, this form was taken to be

$$\theta=(A+Be^{Cx})/\sqrt{p_0}\ \text{cm} \tag{1}$$

where p_0 is in mm Hg abs. and x in cm. The form of this empirical relation was chosen to reflect the expected (and verified) dependence of θ on p_0, as well as the observed rapid increase of θ after the throat. The method of least squares was used to find that $A=0.123$, $B=0.00269$ and $C=0.394$. The measured unit Reynolds number and Eq. (1) were used to plot the transition data, as will be seen subsequently. Additional details on the flow measurement just described are found in Ref. 10.

IV. Roughness Characterization

The study of roughness-induced transition described next was done by attaching strips of sandpaper on the nozzle

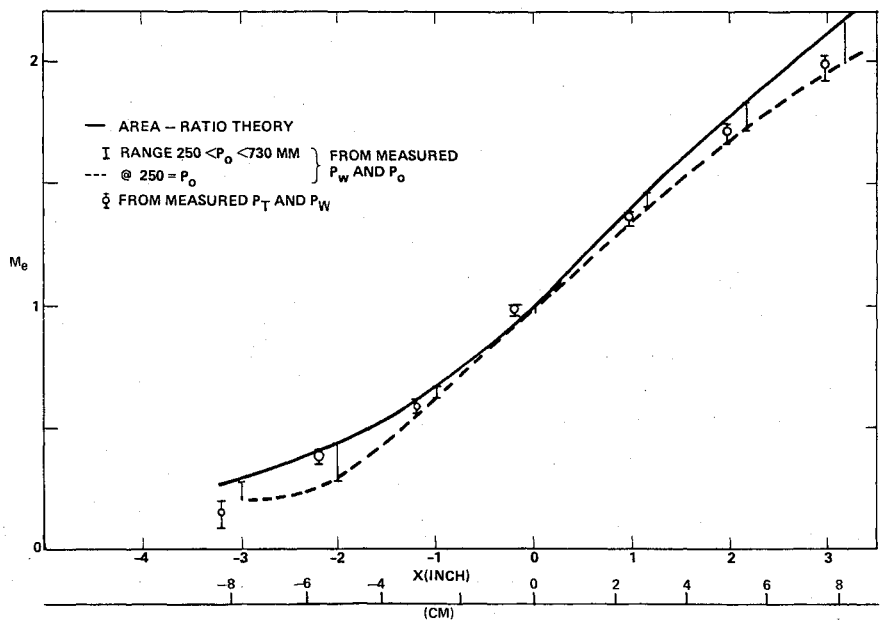

Fig. 3 Edge Mach number distribution.

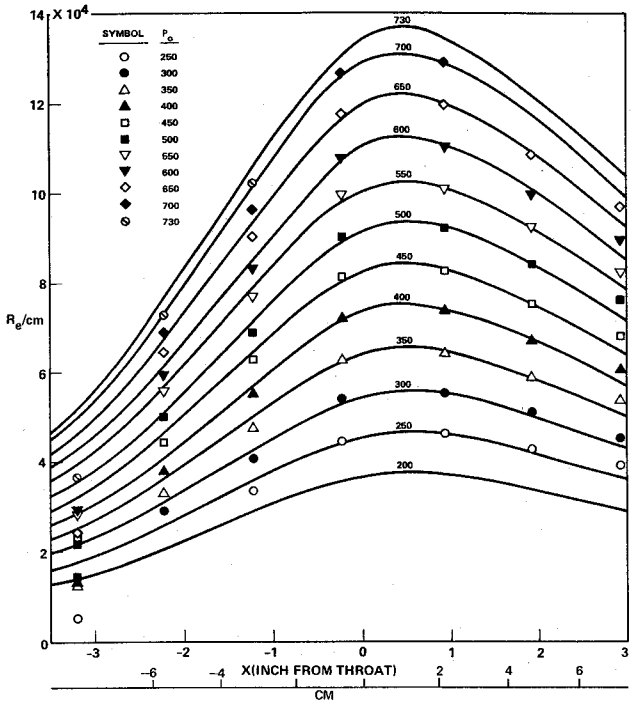

Fig. 4 Measured unit Reynolds number (points) compared with inviscid one-dimensional theory (curves); numbers are in mm Hg abs.

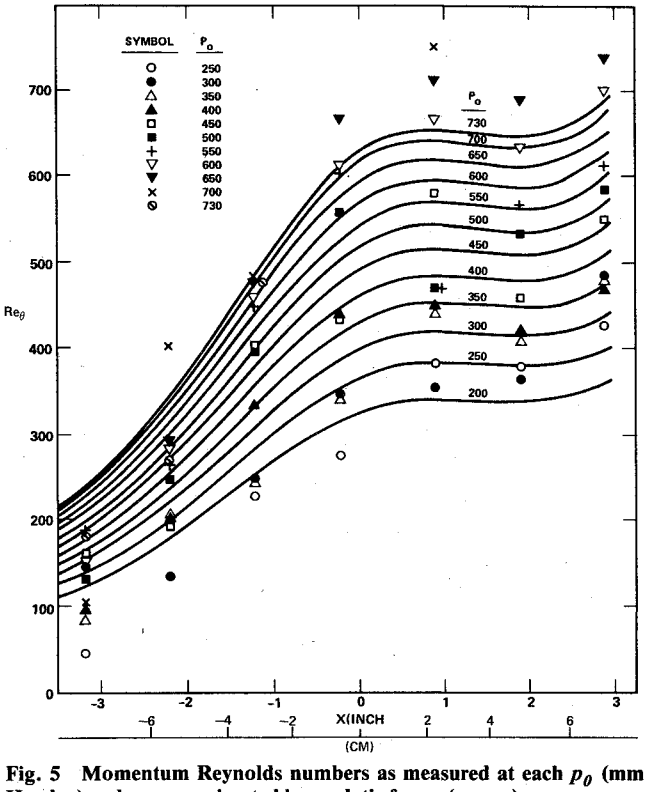

Fig. 5 Momentum Reynolds numbers as measured at each p_0 (mm Hg abs.) and as approximated by analytic forms (curves).

block, spanning the test section and extending from about 14 cm upstream to 14 cm downstream of the sonic throat. In view of the measured smooth-wall boundary-layer thicknesses δ_s which were of order 0.075 cm in the throat region, these "roughness overlays" were thus a few hundred δ_s long and began about 100 δ_s upstream of the farthermost upstream point probed in this experiment.

Nine different shop-quality sandpaper overlays (from 60 to 600 grit) were used which, with the smooth-wall condition,

Table 1 Statistical characteristics of sandpaper roughness

Grit	k, cm	Trace rms, cm[a]	Skewness factor	Flatness factor
60	0.0100	0.0073	−0.912	3.792
80	0.0110	0.0070	−0.217	2.351
100	0.0086	0.0058	−0.731	3.222
120	0.0048	0.0036	−0.221	2.51
220	0.0038	0.0025	−1.03	3.828
280	0.0026	0.0014	−0.896	3.75
320	0.0020	0.0013	−0.999	4.078
400	0.0008	0.00065	−0.303	2.936
600	0.00062	0.00051	−0.028	2.436
		Average:	−0.492	2.79

[a] About the mean.

bring to ten the surface-roughness conditions utilized. The roughness height k was measured from profilometer traces taken for each overlay. The abrasive particles on the materials appeared as a succession of peaks and valleys on the digitized profilometer record; the computer then defined each individual particle height as the height of each peak referred to the valley following it, and averaged all such heights on the trace into the value of k for that overlay. The same computer program also gave statistical properties of the trace such as its arithmetic average, root-mean square, etc..., as well as the skewness and flatness factor. Because of the suitability of sandpaper as a surface-roughness agent, some of these properties are listed on Table 1 on the chance that they may be useful to the reader. Note that the skewness and flatness factors are sufficiently close to their Gaussian values (0 and 3, respectively) to ensure some semblance of randomness in the sandpaper roughness distribution.

V. Transition Measurements

Transition in the boundary layer over the range $-8<x<8$ cm was examined with the smooth wall and with each of the roughness overlays just discussed. The transition detectors were hot-film anemometers designed and fabricated by the author, consisting of glass rods 0.025 or 0.05 cm in diameter with their tips ground to a slender double wedge. The tip of the wedge was a 0.025×0.0025 cm (or 0.05×0.005 cm) strip on which a platinum film was deposited, held normal to the flow, and parallel to the wall surface. Powered by a constant current of order 10 MA and coupled to a hot-wire amplifier with a 0-500 KHz passband, this sensor responds to turbulence with a large ac signal, which in this case was much larger than the circuit noise. A qualitative examination of this signal is adequate to ensure the presence of turbulence, making the hot-film a rugged and convenient means of transition detection.

The detection procedure consisted of keeping the hot film stationary at a fixed x and at a distance $y\simeq\delta/2$ above the wall; the probe support and actuation gear described in the previous section were utilized for this purpose. In this instance the forward support arrangement of Fig. 2 was replaced by a piano-wire "skid" attached to the film probe to suppress tip vibration, allowing more x positions to be sampled for transition detection than were for profile measurements. 136 combinations of x and k were utilized. After positioning of the probe, the tunnel pressure p_0 was swept, i.e., slowly changed, usually from 200 to 730 mm Hg abs., producing local edge unit Reynolds number changes across the range of Fig. 4. Graphic plots of p_0 vs the film rms output were obtained during the sweep, from which the rms signal increase due to transition was used to establish the transition p_0 for that particular combination of x and k. Tests showed that the transition data were quite insensitive to whether p_0 was increased or decreased during the sweep, or to the speed of the p_0 change.

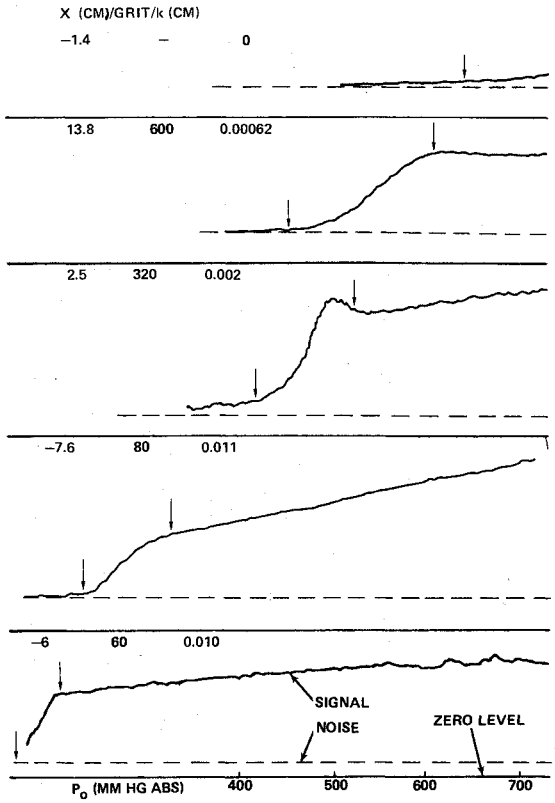

Fig. 6 Typical variation of the rms hot-film anemometer output obtained by sweeping p_0. Note variation of signal-to-noise ratio across the transition zone bracketed by the pair of arrows.

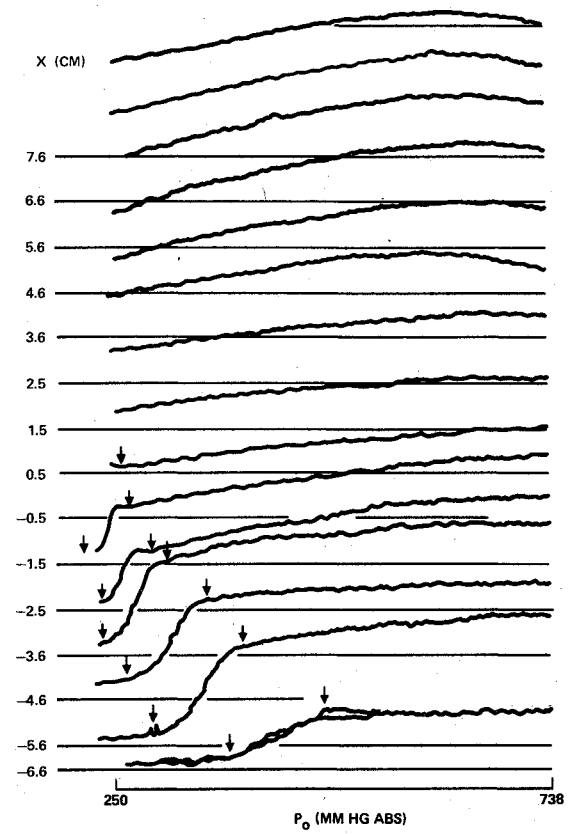

Fig. 8 The hot-film anemometer rms output vs p_0 for the 120-grit case; $k = 0.0048$ cm.

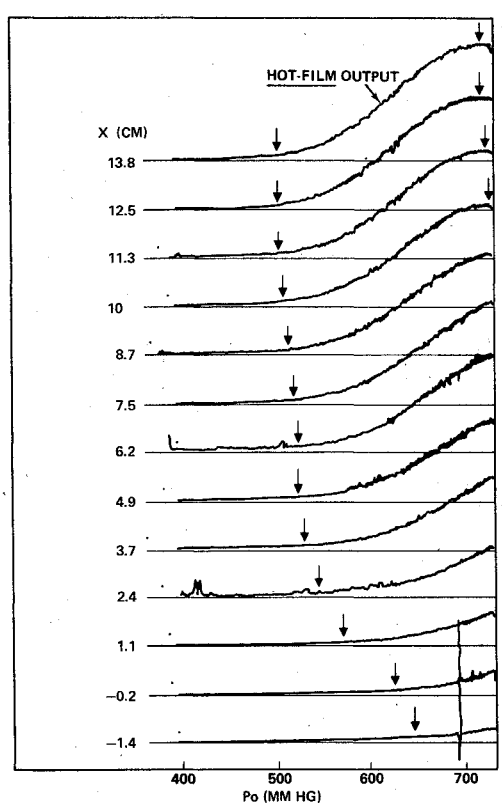

Fig. 7 Variation of the hot-film anemometer rms output with p_0 for the smooth wall.

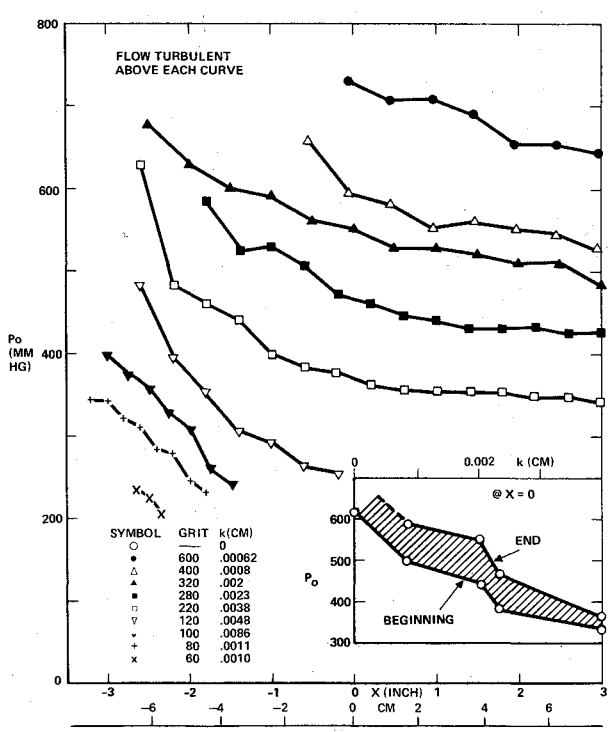

Fig. 9 The end-of-transition pressures vs distance along the nozzle. Similar beginning-of-transition data define the transition zone extent shown shaded in the inset plot of p_0 vs k.

Typical results are shown on Figs. 6-8. In Fig. 6 we illustrate the general form of the probe signal "signatures" in which the signal is indistinguishable from the electronic noise when the flow is laminar, but rises and becomes much larger than the noise in the turbulence. The arrows demonstrate how the p_0 for "beginning" and "end" of transition (p_{0B} and p_{0E}, respectively) were chosen. Note the small qualitative differences from one signature to the next, such as the "overshoot" in the case $x = 2.54$ cm with the 320-grit overlay. Tests showed that these differences were due to slight differences in the vertical distance y from the wall, but that p_{0B} and p_{0E}

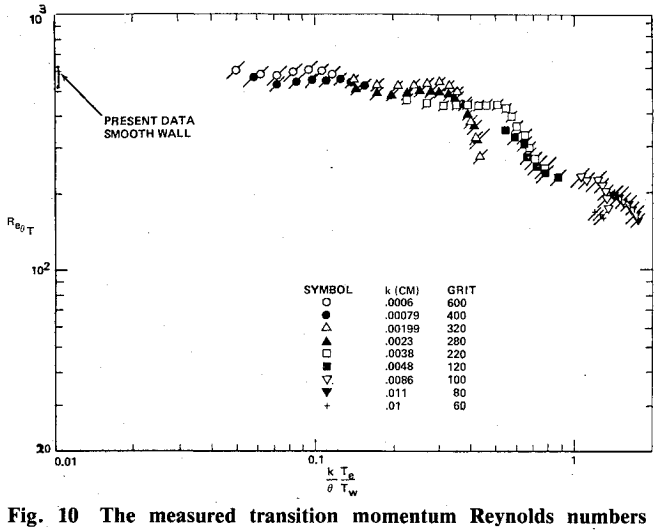

Fig. 10 The measured transition momentum Reynolds numbers plotted as a function of the nondimensional roughness height.

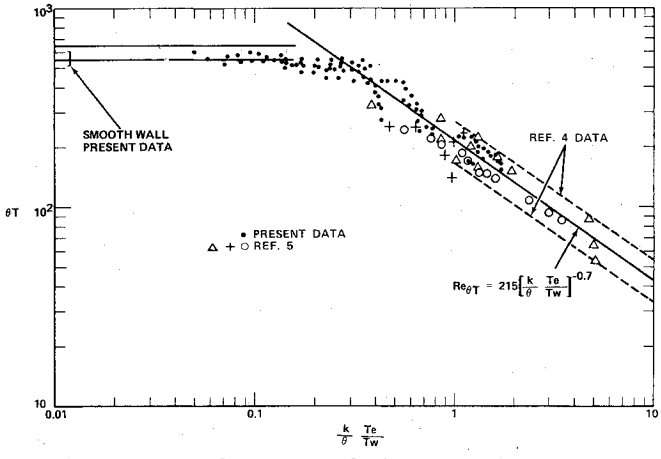

Fig. 11 The present data compared with data on blunt bodies in windtunnels at hypersonic speeds.

themselves were insensitive to y so long as $y<\delta$. Figures 7 and 8 illustrate two extreme groups of the data, in which transition barely gets to the throat at the highest attainable pressures with the smooth nozzle surface (Fig. 7) but always covers the throat with a turbulent boundary layer for the 120-grit overlay (Fig. 8). When plotted vs x, the beginning and end pressures assume a variation such as shown on Fig. 9. The inset of this figure plots p_{0B} and p_{0E} vs k at a fixed x, to demonstrate that the transitional zone is rather limited to an increment less than about 100 mm Hg. Typical transitional flow lengths were of order 30 boundary-layer thicknesses.

VI. Discussion of the Transition Data

From the preceding we have seen that boundary-layer transition advances upstream when either the supply pressure p_0 or the surface roughness height increases, or when both increase. Having available the variation of Re_θ as a function of x and p_0 from Fig. 5, it is possible to cast these data in a variety of forms. In Figs. 10 and 11, the data are shown in the form of the transition momentum Reynolds number vs the nondimensional roughness height $\bar{k}$ proposed by Anderson and his co-workers for boundary-layer transition on blunt bodies.[4] The extremities of each line shown passing through each datum point on Fig. 10 define the beginning and end Re_θ corresponding to p_{0B} and p_{0E}. The present smooth-wall transition data ($\bar{k}=0$) are indicated by an asymptotic mark on the vertical axis. Figure 10 seems to indicate that in this wind tunnel the transition Re_θ is insensitive to $\bar{k}$ when $\bar{k}<0.1$ and only weakly dependent on $\bar{k}$ until $\bar{k}=0.4$.

The present data are compared on Fig. 11 with blunt-body transition data presently available in Refs. 4 and 5, as well as with the empirical correlation of Anderson and his co-workers[4]

$$Re_{\theta T}=215\left[\frac{k}{\theta}\,\frac{T_e}{T_w}\right]^{-0.7} \tag{2}$$

It is clear from this figure that there is agreement among the three experiments, subject to the departure of $Re_{\theta T}$ from the former correlation at small $\bar{k}$. The same behavior is noted on Fig. 12 when all three experiments are compared with the correlation of Van Driest[11] who introduced the "stablizing" influence of the surface curvature, here appearing in the denominator of the abscissa. Most significantly, a similar trend is observed to occur on Fig. 13 where the viscosity of the momentum Reynolds number of transition is evaluated at the wall, and where the mass flux $\rho_k u_k$ is considered at the height of the roughness element. The importance of this correlation, which is basically due to Dirling[13] except for the curvature correction, lies in the inverse proportionality

$$\rho_e u_e \theta/\mu_w \doteq \text{const.}\,(\rho_k u_k k/\rho_e u_e \theta)^{-1} \tag{3}$$

which the data of Ref. 4 and 12 were found to obey in this plot.† The relation Eq. (3) implies that

$$Re_k \equiv \rho_k u_k k/\mu_w = \text{const.} \tag{4}$$

as originally proposed by Schiller[14] and later confirmed by Smith and Clutter as the critical Reynolds number above which roughness is effective in promoting transition.[15]

Figures 10-13 thus indicate that the present data can be generally separated into two groups. The group at the larger k is in good agreement with the data of Refs. 4 and 5 and, as Fig. 13 also shows, with the new ballistic-range data of Reda.[12] This agreement (within the scatter) is most interesting, especially in view of the wide diversity among these four experiments with regard to the test set-ups, the type of models, and the methods of measurement. For example, in Ref. 4, the transition measurements were done with surface heat-transfer detection on a blunt body in short-duration flow; in Ref. 5 with hot-wire anemometers, surface thermocouples, and microphones in a different, continuous-flow wind tunnel; in Ref. 12 by in-flight temperature-contour photography of blunt projectiles in a ballistic range; and in the present case with the film anemometer in a DeLaval throat region. Depending on which group of data was considered at the time, finite but small differences in the numerical constant in Eqs. (3) and (4) have been reported; it was found to be 160 by Dirling,[13] 186 by Finson,[16] 192 by Reda,[12] and in the present case it seems to be about 200. Therefore, within these limits and as a consequence of the evidence presented in Figs. 10-13, the highly favorable pressure gradient and the curvature along the supersonic nozzle throat appear capable of simulating the boundary-layer transition characteristics on the forward part of blunt bodies at high speeds.

The second subdivision of the present data, extending to the left margin of each of Figs. 10-13, were taken mainly in the supersonic portion of the nozzle toward the Mach 3 test section and at small physical roughness heights. These data should therefore depart from the various "blunt body roughness correlations" mentioned, and should approach asymptotically the transition Reynolds number characteristic of the prevailing flow properties on the test section walls of

†Dirling's original correlation included a curvature-correcting factor similar to that supplied by Van Driest. Figure 13 follows Reda's suggestion that the omission of this factor (which is very close to unity for the present data) actually improves the agreement between his data and those of Ref. 4.

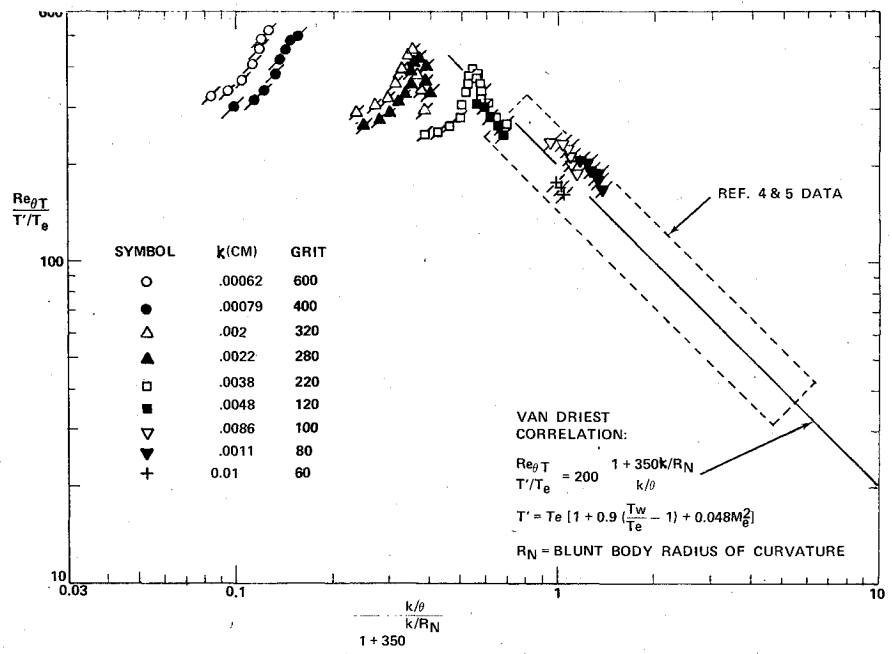

Fig. 12 Plot of the present transition data, according to the Van Driest correlation.[11]

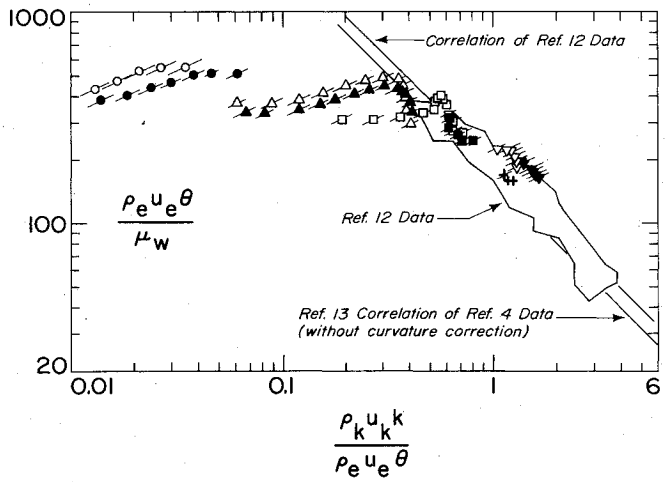

Fig. 13 Plot of the present transition data according to the method proposed by Reda[12] showing Reda's data and Dirling's correlation without curvature correction (see Fig. 12 for key to symbols).

the particular windtunnel employed; a similar behavior might be expected for the boundary layer of a blunt body faired to a frustum in the downstream direction. These flow properties, of course, include the freestream turbulence intensity since the latter can affect transition on the smooth test section walls, and thus also the $k=0$ asymptote in the context of Figs. 10-13. In the configuration employed here the transition (momentum) Reynolds number over an adiabatic, smooth, flat plate in the Mach 3 test section[9] is of order 600 and this is confirmed by the data asymptote of Figs. 10 and 11.

Summarizing the preceding remarks and considering the present as well as the previously reported data, it appears that the combination of large roughness height, strong favorable pressure gradient, and perhaps also curvature imposes a common behavior on the phenomenon regardless of the method of generating the boundary layer and thus, in a way, regardless of the stream turbulence. This can be called the "roughness-dominated" regime since the transition behavior agrees with the constant roughness Reynolds number (for transition) defined in Eq. (4), as well as the roughness-oriented explanations of transition advanced in Refs. 4, 13, 15 and 16. At the smaller values of the roughness parameters defined in the latter correlations, transition, for the data discussed here, has moved to locations where other influences, e.g., the edge Mach number and the stream turbulence, become paramount; this is a "facility" or, more properly, a "configuration" dominated regime.

VII. Conclusion

The following can be concluded from the work just described.

1) Transition to turbulence in the boundary layer covering th throat region investigated can be caused to move upstream when the height of distributed random roughness is increased, or when the supply pressure is increased, or both.

2) The present data which fall within the range of the roughness parameter in which data from blunt-body transition tests are available agree with such blunt-body experimental results, endorsing the likelihood of simulating the blunt-body transition phenomenon with the nozzle set-up utilized here. In this roughness-dominated regime the present results agree with empirical correlations devised for blunt-body boundary-layer transition and with earlier proposals for a critical roughness Reynolds number.

3) As the roughness parameter decreases, the present data were found to depart from the abovementioned correlations and to join smoothly with the transition Reynolds numbers observed on smooth walls of the test section of this wind tunnel. The generality of this portion of the data is then obviously restricted by the conditions in the test section including its design Mach number and stream turbulence.

Acknowledgments

This work was performed under Air Force Contract FO 4701-77-C-0113 while the author was at the Aeronutronic Division of the Ford Aerospace and Communications Corporation.

References

[1]Pate, S. R., "Dominance of Radiated Aerodynamic Noise on Boundary Layer Transition in Supersonic-Hypersonic Wind Tunnels: Theory and Application," Ph.D. Thesis, University of Tennessee, Knoxville, Tenn. March 1977

[2]Reshotko, E. "A Program for Transition Research," *AIAA Journal*, Vol. 13, March 1975, pp. 261-265.

[3] Harvey, W. D., Stainback, P. C., Anders, J. B., and Cary, A.M., "Nozzle Wall Boundary-Layer Transition and Freestream Disturbances at Mach 5," *AIAA Journal,* Vol. 13, March 1975, pp. 307-314.

[4] Anderson, A. D., "Passive Nosetip Technology (PANT) Program, Interim Report, Volume X: Boundary-Layer Transition on Nosetips with Rough Surfaces," U. S. Air Force SAMSO, Los Angeles, Calif. TR 74-86, Jan. 1975.

[5] Laderman, A. J., "Effect of Surface Roughness on Blunt Body Boundary-Layer Transition," *Journal of Spacecraft and Rockets,* Vol. 14, April 1977, pp. 253-255.

[6] Deveikis, W. D. and Walker, R. W., "Local Aerodynamic Heat Transfer and Boundary Layer Transition on Roughened Sphere-Ellipsoid Bodies at Mach Number 3," NASA TN D-907, Aug. 1961.

[7] Chambre, P. L. and Schaaf, S. A., "The Impact Tube," *Physical Measurements in Gas Dynamics and Combustion,* edited by R. W. Ladenburg, Princeton University Press, Princeton, N.J., 1954, pp. 111-122.

[8] Demetriades, A., "Mean Flow Measurements in an Axisymmetric Compressible Turbulent Wake," *AIAA Journal,* Vol. 6, March 1968, pp. 432-439.

[9] Laderman, A. J., "Effect of Wall Temperature on a Turbulent Supersonic Boundary-Layer," *AIAA Journal,* Vol. 16, July 1978, pp. 723-729.

[10] Demetriades, A., "Roughness-Induced Transition on a Blunt Body Simulated by a DeLaval Nozzle Throat," Aeronutronic Rept. U-6496, Newport Beach, Calif., 1977-78.

[11] Van Driest, E., private communication, Aerospace Corporation, Los Angeles, Calif. 1977-78.

[12] Reda, D. C., "Correlation of Nosetip Boundary-Layer Transition Data Measured in Ballistics-Range Experiment," AIAA Paper 80-0286, Pasadena, Calif. Jan. 1980.

[13] Dirling, R. B. Jr., Swain, C. E., and Stokes, T. R., "The Effect of Transition and Boundary-Layer Development on Hypersonic Reentry Shape Change," AIAA Paper 75-673, Denver, Colo., May 1975.

[14] Schiller, L., *Handbuch der Experimentalphysik,* Vol. 4, Pt. 4, Leipzig, 1932.

[15] Smith, A. M. O. and Clutter, D. W., "The Smallest Height of Roughness Capable of Affecting Boundary-Layer Transition," *Journal of the Aerospace Sciences,* Vol. 26,April 1959, pp. 229-245.

[16] Finson, M. L., "An Analysis of Nosetip Boundary Layer Transition Data," AFOSR Rept. TR-76-1106, Aug. 1976.